PROBE METHODS FOR DIRECT MEASUREMENTS OF THE PLASMA POTENTIAL★

R. SCHRITTWIESER[1], C. IONIȚĂ[1], P. C. BALAN[1], C. A. F. VARANDAS[2], H. F. C. FIGUEIREDO[2], J. STÖCKEL[3], J. ADÁMEK[3], M. HRON[3], J. RYSZAWY[3], M. TICHÝ[4], E. MARTINES[5], G. VAN OOST[6], T. KLINGER[7], R. MADANI[7]

[1] Association EURATOM/ÖAW, Department of Ion Physics, University of Innsbruck, Austria
[2] Association EURATOM/IST, Centro de Fusão Nuclear, Instituto Superior Técnico, Lisboa, Portugal
[3] Institute for Plasma Physics, Association EURATOM-IPP.CR, Czech Academy of Sciences, Prague, Czech Republic
[4] Faculty of Mathematics and Physics, Charles University in Prague, Czech Republic
[5] Consorzio RFX, Associazione EURATOM-ENEA sulla Fusione, Padova, Italy
[6] Department of Applied Physics, Ghent University, Belgium
[7] Max Planck Institute for Plasma Physics, Greifswald Branch, EURATOM Association, Germany

Received December 21, 2004

One of the most important plasma parameters is the plasma potential Φ_{pl}. In this review a survey is given of two probe methods, by which the plasma potential can be measured directly since the floating potentials of the probes become equal to Φ_{pl}. There are two ways to achieve that: (i) to increase the positive probe current, or (ii) to reduce the negative probe current. The first method is realized in the electron-emissive probe whose floating potential is almost equal to Φ_{pl} when the emission current becomes approximately equal to the electron saturation current. The second method can only be applied in a magnetic field where the gyroradii of the electrons are much smaller than those of the ions. Therefore it is possible to screen off a well-defined part of the electron current by a kind of shield in front of the probe collector until it becomes equal to the ion saturation current, whereas the ions can pass by the barrier almost unhindered.

Key words: plasma diagnostic, electric probes, emissive probes, plasma potential, floating potential.

1. INTRODUCTION

Among the most important plasma parameters is the electric space potential of the plasma which is usually called the plasma potential Φ_{pl}. Since potentials can only be determined with respect to a certain reference potential, in a plasma device usually the wall or one of the electrodes of the discharge that produces the

★ Paper presented at the 5th International Balkan Workshop on Applied Physics, 5–7 July 2004, Constanța, Romania.

Rom. Journ. Phys., Vol. 50, Nos. 7–8, P. 723–739, Bucharest, 2005

plasma is used for this purpose. Naturally also this potential is given by Poisson's equation, where the charge density $\rho = e(n_i - n_e)$ is due to the presence of free positive and negative charge carriers (with the number densities $n_{i,e}$ of ions and electrons, respectively) assuming a conventional plasma with electrons and only single-charged positive ions:

$$\Delta\Phi_{pl} = -\frac{\rho}{\varepsilon_0} = -\frac{\rho}{\varepsilon_0}\left(n_i - n_e\right). \tag{1}$$

We emphasize that the plasma potential only depends on the densities of the ions and electrons but not on their velocity distribution, and thus also not on possible particle drifts due to currents or beams. On the other hand, a gradient of Φ_{pl} produces an electric field which gives of course rise to corresponding charge carrier drifts.

In general, the spatial profile and the temporal evolution of the plasma potential are decisive not only for the overall stability of a plasma but also for the loss of plasma across the magnetic field, especially in the case of a magnetically confined plasma such as in toroidal fusion experiments, which on the long run are expected to make possible the gain of energy. Very important in this context is the electric field and its fluctuations in the edge region of such a plasma.

For instance, it has been shown that the transition from the low-density mode (L-mode) to the high-density mode (H-mode) of a tokamak is, among other phenomena, also related to a strong variation of the radial electric field [1–5]. The radial transport of particles in the edge region of a magnetized plasma torus is mainly related to the fluctuation-induced particle flux Γ, which may account for a large part of the anomalous energy and particle losses observed.

A counteracting mechanism might be the Reynolds stress R_e, which is a measure of the anisotropy of turbulent velocity fluctuations. These produce a stress on the mean flow causing a poloidal flow [6–8] if the Reynolds stress has a gradient. The poloidal flow will be sheared, which can reduce the radial turbulent transport [8]. This mechanism plays a key role in explaining the L-H transition and has indeed been found to reduce plasma losses [9].

Both, the fluctuation-induced flux and the Reynolds stress are related to the fluctuations of the electric field in the edge region of a tokamak. One of the best methods to determine these fluctuations at present is to measure the plasma potential directly on appropriate locations by various sets of probes and calculating the difference between the respective values of Φ_{pl}, taking into account the distances between the probes [10–12].

These are just two examples why it is vital to measure the plasma potential directly and as fast as possible with a good spatial and temporal resolution. In the following we will describe two different probe methods for this purpose.

2. BASIC FACTS ABOUT PROBES

The simplest, least expensive and easiest to handle plasma diagnostic tools are cold plasma probes which are known since their first description [13, 14]. A cold probe (also called Langmuir probe) consists of a small electrode of various forms which is inserted into the plasma and externally biased with respect to the plasma potential. However, since the plasma potential is not directly accessible, the bias has to be applied with respect to the external reference electrode. A probe is called "cold" as long as it only passively registers the charge carrier fluxes towards it, but does not emit particles. These fluxes depend on the surrounding plasma, on the probe bias V_p, on the form of the electrode, and on a possible magnetic field.

The solid line in Fig. 1 shows a typical current-voltage characteristic, $I_p = I_p(V_p)$, of a cold probe in a conventional plasma, consisting of electrons and single-charged positive ions, where both particle species have Maxwellian velocity distributions. The other two characteristics (dashed line and dotted line) will be explained below.

As we can see, the characteristic is asymmetric, since the ion saturation current is much smaller than the electron saturation current. Therefore the floating potential V_{fl} of such a probe is more negative than the plasma potential Φ_{pl}. The reason for the strong discrepancy between the currents lies in the fact that the electrons have a much smaller mass than the ions and therefore a much

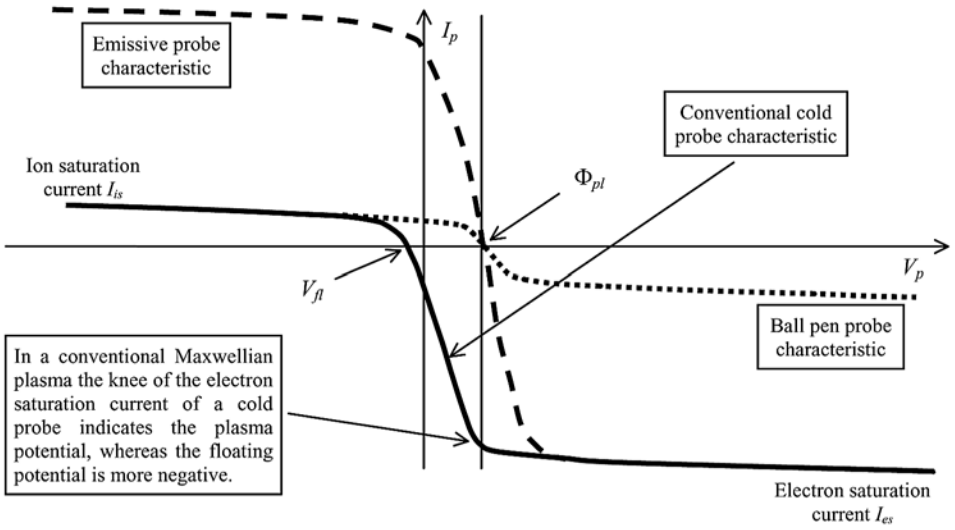

Fig. 1. – Typical current-voltage characteristics of a cold probe (solid line), of an emissive probe (dashed line), and of a ball-pen probe (dotted line) in a plasma with Maxwellian velocity distributions for the electrons and ions. Concerning the two latter probe types see below.

higher mean velocity and average flux than those of the ions. The average current density of electrons and ions in a conventional unmagnetized plasma is given by:

$$j_{i,e} = \pm \frac{en_{i,e}\overline{v}_{i,e}}{4} = \pm \frac{en_{i,e}}{2}\sqrt{\frac{2eT_{i,e}}{\pi m_{i,e}}}, \tag{2}$$

where $\overline{v}_{i,e}$ are the mean velocity of ions and electrons, $T_{i,e}$ the ion and electron temperature (to be taken in eV) and $m_{e,i}$ the electron and ion mass, respectively.

Thus practically always $j_e >> j_i$ (unless $T_i >> T_e$, which is very seldom the case; on the contrary, in a normal gas discharge plasma $T_e >> T_i$!). We note here that Eq. (2) does not yield the true value for the ion saturation current density, which should rather be calculated taking into account the ion acoustic velocity, but for our basic consideration it suffices.

The fact that the electron flux is higher than that of the ions in the overwhelming majority of plasmas has the effect that any electrode, which is in touch with a plasma and which carries no current, becomes negatively charged; or vice-versa, the plasma adjusts itself on a positive value with respect to the electrode.

The relation between the floating potential of a cold probe and the plasma potential in the case of a conventional Maxwellian plasma is well known from simple probe theory:

$$\Phi_{pl} = V_{fl} + T_e \ln\left(\frac{I_{es}}{I_{is}}\right). \tag{3}$$

We see that when the electron temperature T_e is known, it is in principle sufficient to measure the floating potential of a cold probe, and the plasma potential can be calculated. However, on one side is it not so easy to measure T_e with sufficient accuracy, on the other side T_e can fluctuate during the measurement and there can be temperature gradients in the region of investigation, which is always the case in the edge region of a hot magnetized plasma. Moreover, also the ratio between the ion and the electron saturation currents I_{es}/I_{is} cannot always be determined precisely, especially in a strong magnetic field [15].

An additional, often ignored fact is that the entire characteristic of a cold probe shifts to the negative side and will therefore deliver erroneous results for the plasma potential whenever there is a stronger deviation of the electron velocity distribution function from a Maxwellian one, for instance when there is an electron drift or an electron beam or runaway electrons.

In the following two chapters we will discuss two possibilities, by which the floating potential of a probe can be shifted to become equal to the plasma potential, thereby enabling a direct measurement of Φ_{pl}. Such a probe can, however, no longer be a simple cold probe.

3. PROBES FOR DIRECT PLASMA POTENTIAL MEASUREMENTS

From the two other characteristics in Fig. 1 we see that the floating potential of a probe becomes identical to Φ_{pl} when the characteristic is symmetric. This can also be proven theoretically. We note here that a symmetric characteristic will also be yielded in the case of a plasma that consists of positive and negative ions of similar mass but no electrons. In this case, provided that the two ion species have also similar temperatures, from Eq. (2) follows that the fluxes become equal. But in the case of a conventional electron-positive ion plasma, we have to resort to other means.

In principle there are two ways to achieve an equality of the current on both sides of the characteristic and thereby a shift of the floating potential towards the plasma potential:

- Either we compensate the plasma electron saturation current by an almost equally strong current on the negative (left-hand) side of the characteristic (dashed line in Fig. 1),
- Or we reduce the plasma electron saturation current on the positive (right-hand) side of the characteristic, until it becomes equal to the ion saturation current (dotted line in Fig. 1).

In the following the two types of probe are discussed and typical results are presented.

3.1. EMISSIVE PROBES

3.1.1. Emissive wire probe

An electron emissive probe is usually realized by a small half-loop of tungsten or thoriated tungsten wire of a diameter of 0.2 mm. The two ends of this half-loop are pulled through the two bores of a double-bore ceramic tube and are at the other end connected by feed-throughs to an external power supply. Thus the loop can be heated to the necessary temperature (white glow $\cong$ 2500 K). In order to heat only the protruding tungsten wire loop, we have devised a method to increase the conductivity of the wires inside the bores, which prevents the heating therein. For more details see [15, 16, 17].

When such a probe is inserted into a plasma and heated sufficiently, in the current-voltage characteristic the electron emission current I_{em} is observable on top of the ion saturation current I_{is} (cf. the dashed line in Fig. 1). This is due to the fact that a current of electrons emitted from the probe has the same sign as the current of positive ions flowing from the plasma to the probe. An emission current can flow as long as the bias of the probe is more negative than the plasma potential. For increasing probe heating, the current on the left-hand side of the characteristic increases while the floating potential shifts to the right-hand side

towards the plasma potential until a kind of saturation of this value is reached, and further heating will be to no avail. Then this value is assumed to be a sufficiently good approximation of Φ_{pl} and is henceforth measured directly with a high-impedance data acquisition system, while the heating is maintained. Fig. 2 shows a schematic presentation of an emissive wire probe together with the heating circuit.

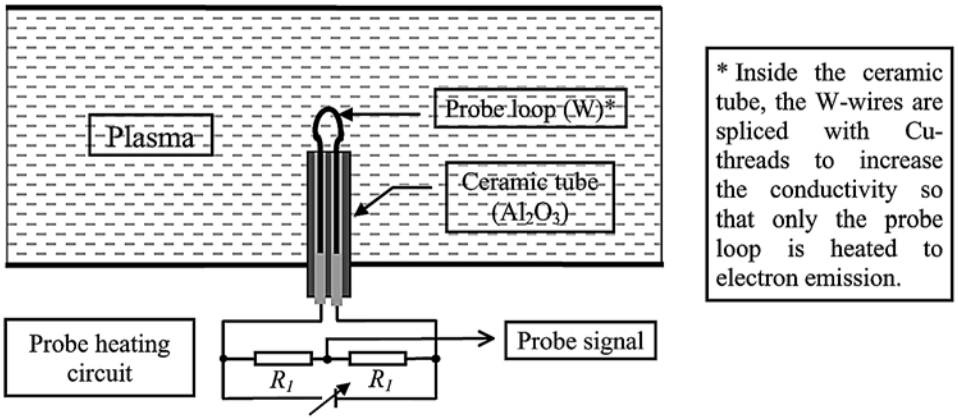

Fig. 2. – Schematic presentation of an emissive probe inside the plasma together with the heating circuit.

The theory of the determination of Φ_{pl} by an emissive probe is the following: if the probe is heated externally until electron emission, the total probe current I_p, as a function of the probe voltage V_p, is given by $I_p(V_p) = I_i + + I_{em} - I_e$, where $I_{i,e}$ are the ion and electron currents (not necessarily the saturation values).

We are only interested in the part of the characteristic up to the plasma potential, *i.e.*, $V_p \leq \Phi_{pl}$, where the electron current is space charge limited. Then for the ion and electron currents we have to insert:

$$I_s = I_{is} \tag{4a}$$

and

$$I_e = I_{es} \exp\left(\frac{V_p - \Phi_{pl}}{T_e}\right), \tag{4b}$$

Then, for a Maxwellian plasma, the floating potential of the probe can be calculated by putting $I_p = 0$, and an analogous equation as Eq. (3) can be derived:

$$\Phi_{pl} = V_{fl,em} + T_e \ln\left(\frac{I_{es}}{I_{is} + I_{em}}\right). \tag{5}$$

Here $V_{fl,em}$ is the actual floating potential of the probe which depends mainly on the emission current. Since we are interested in the difference between the floating potential of the emissive probe and the plasma potential, we define Δ as follows:

$$\Delta \equiv \frac{V_{fl,em} - \Phi_{pl}}{T_e} = \ln\left(\frac{I_{is} + I_{em}}{I_{es}}\right). \tag{6}$$

For the emission current we have to insert Richardson's emission law:

$$I_{em} = A_{em} A^* T_w^2 \exp\left(-\frac{eW_w}{k_B T_w}\right), \tag{7}$$

with A_{em} being the emitting area, A^* the Richardson constant, T_w the temperature of the wire (in K) and W_w the work function of the wire material. For tungsten $A^* \cong 6\times10^5$ Am^{-2}K^{-2} and $W_w = 4.55$ eV.

From Eq. (5) we see that for increasing emission current I_{em}, the second term decreases and vanishes for $I_{em} = I_{es} - I_{is}$, while Δ in Eq. (6) becomes zero. Thus when the emission current just compensates the electron saturation current (minus the ion saturation current, but this is usually negligible), the floating potential of such a probe equals the plasma potential: $V_{fl,em} = \Phi_{pl}$.

Fig. 3a shows the decrease of the magnitude of Δ (here negative for reasons of better clarity) with increasing emission current normalized to the ion saturation current. We see that for $I_{em}/I_{is} \cong 11$ the difference reaches zero, *i.e.*, $V_{fl,em} = \Phi_{pl}$. For this theoretical consideration we had to make an assumption of $I_{es}/I_{is} = 12$, which means that the ion saturation current is about 8% of the electron saturation current. This value depends on $T_{i,e}$ and on the magnetic field, which determines the effective probe area for ion and electron collection and is therefore partly questionable.

This simplified treatment is true only for Maxwellian electrons, but it can be shown that also for drifting electrons the floating potential of an emissive probe is sufficiently near the plasma potential, however, in this case $I_{em} > I_{es}$.

Fig. 3b shows samples of results of an experiment in the CASTOR tokamak with an emissive probe in the edge region where the plasma density was about 10^{18} m^{-3} and the electron temperature $T_e \cong 10$ eV [15]. CASTOR has a major radius of 40 cm and a minor radius of about 8.5 cm. The magnetic field is 1 T and the plasma current 10 kA. Shown is also the difference Δ as function of I_{em}/I_{is} at two different radial positions (one inside, one outside the last closed flux surface, which is at $r = 7.8$ cm), but here $\Delta = (V_{fl,em} - V^*_{fl,em})/T_e$ is the difference between the actual floating potential of the probe $V_{fl,em}$ (depending on

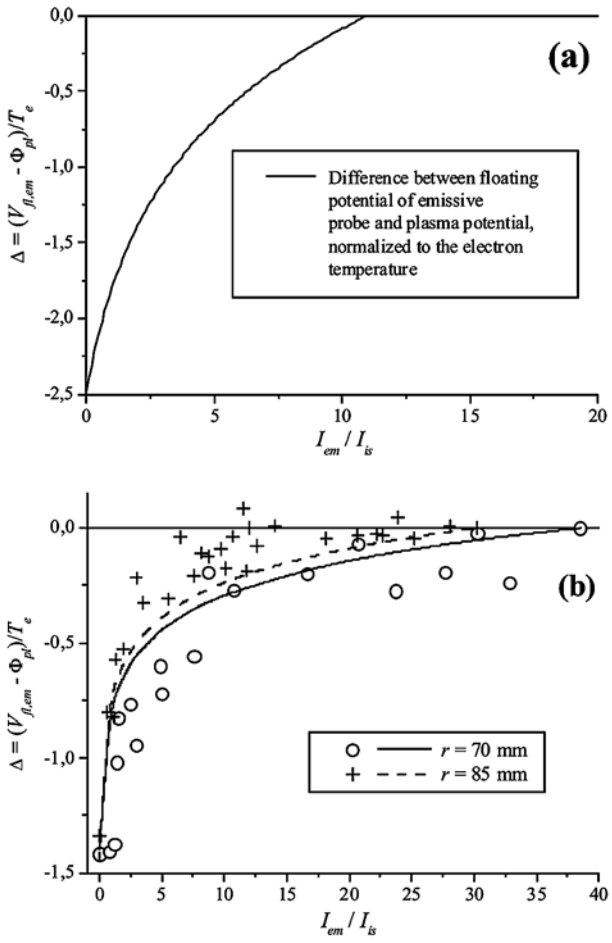

Fig. 3. – (a) Approach of the floating potential of an emissive probe to the plasma potential according to Eqs. (5, 6) with increasing emission current; (b) Comparative results from an experiment in the CASTOR tokamak in Prague at two radial positions in the edge plasma region.

the actual emission current) and the saturation value attained for strong heating $V^*_{fl,em}$, *i.e.*, for about $I_{em}/I_{is} \geq 20$. The electron temperature was determined in the usual way for both radial positions from the characteristic of the unheated probe. Also I_{is} was taken from the cold characteristic. $V^*_{fl,em}$ is assumed to be the true value of Φ_{pl}.

The results of Fig. 3b show a good qualitative agreement with Fig. 3a. Starting from a cold floating potential of $V_{fl} \cong +13$ V, $V_{fl,em}$ increases up to a saturation value of $V^*_{fl,em} \cong +45$ V. There is, however, a discrepancy to the value of $\Phi_{pl} \cong +56$ V determined from the cold characteristic. This corresponds to the discrepancy between the maximum value of Δ, which is –2.5 in the theoretical case (Fig. 3a) and about –1.4 in the experiment (Fig. 3b). This effect is not yet

completely clarified, but seems to be due to a space charge of emitted electrons around the probe, which cannot leave the probe even for $V_p \leq \Phi_{pl}$ due to their much lower temperature (corresponding to the wire temperature $T_w \cong 0.2$ eV) than the plasma electrons ($T_e \cong 10$ eV). This pulls the floating potential below Φ_{pl} [15, 18]. In the case of the CASTOR measurements this leads to the effect that $V^*_{fl,em}$ remains about $1.1T_e$ below the value of Φ_{pl} determined from the cold probe characteristic.

The floating potentials of Fig. 3b were taken from successive measurements of the characteristic for increasing probe heating current during a series of shots of CASTOR. Fig. 4 shows examples of such characteristics where the increase of the probe current on the negative side of the characteristic and the corresponding shift of the floating potential to the right is clearly visible. The lowermost characteristic (crosses) was taken without probe heating, therefore it shows the cold characteristic from which T_e and I_{is} were determined. The uppermost characteristic (triangles) was taken for strongest probe heating.

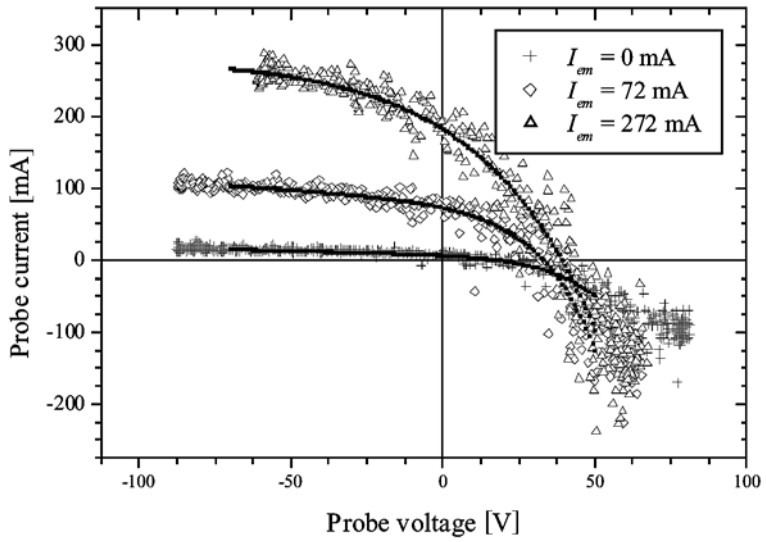

Fig. 4. – Three typical probe characteristics from CASTOR tokamak in Prague in the edge plasma region for increasing probe heating and thus emission current, which is indicated.

3.1.2. Laser-heated emissive probe

Fig. 5a,b show similar results as Figs. 4 and 3b, respectively, from a very recent investigation at the VINETA plasma machine at the Max Planck Institute, Greifswald Branch, Germany [19]. This device produces an argon plasma of

10 cm diameter and 4 m length in a magnetic field of 0.1 T with a density of about 10^{19} m^{-3}, an electron temperature of 3 eV and an ion temperature of 0.2 eV. The plasma is produced by a helicon discharge of less than 6 kW [20].

The probe consists of a cylindrical piece of lanthanum hexaboride, LaB_6, with a diameter of 3.2 mm and a height of 2.2 mm. The LaB_6 electrode is connected to a molybdenum wire of 0.2 mm diameter. The Mo-wire was spliced with a number of copper threads and pulled through a one-bore ceramic tube to provide the electrical connection. The LaB_6 electrode is heated by an infrared high-power diode laser JenLas HDL50F from the company JenOptik, Jena, Germany, with a maximum output power of 50 W and a wavelength of 808 nm. The laser beam is coupled to a conventional glass fibre of about 3 m length that ends in a lens head, by which, in a distance of 15 cm, a focus of 0.6 mm diameter can be produced. This laser-head was positioned directly on a quartz-glass window perpendicular to the direction of the probe insertion.

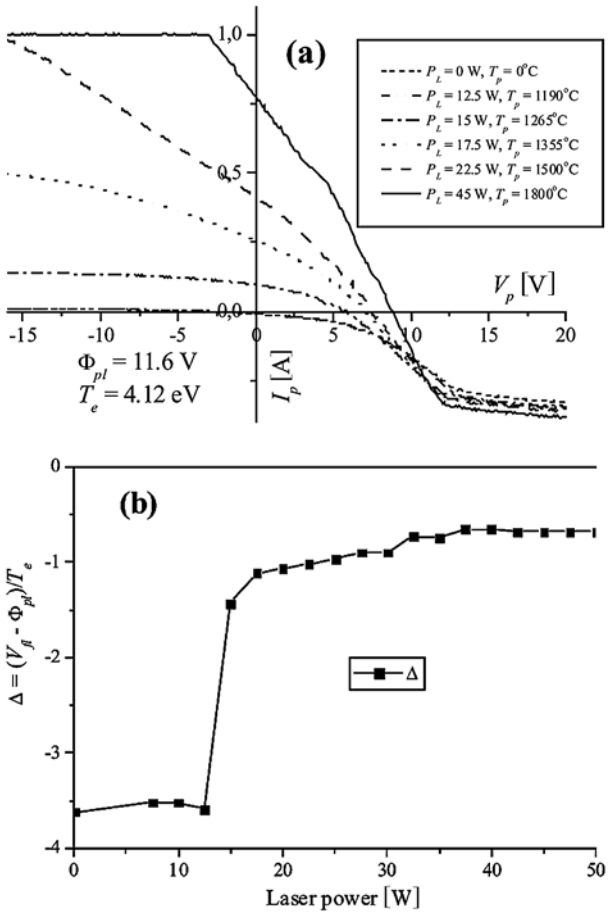

Fig. 5. – (a) Typical probe characteristics from the VINETA device in Greifswald for increasing probe heating by laser irradiation; the laser power and the corresponding temperature of the probe are indicated; (b) Approach of the floating potential of the laser heated emissive probe to the plasma potential versus the laser heating power.

From Fig. 5a we see that also the laser-heated emissive probe shows the same typical behavior as a conventional emissive wire probe, *i.e.*, the emission current supersedes the ion saturation current while the floating potential shifts to the right-hand side. The inserted values of the electron temperature, $T_e = 4.12$ eV, and the plasma potential, $\Phi_{pl} = +11.6$ V, have been determined from the cold *I–V* characteristics (for $P_L = 0$ W) for comparison. Fig. 5b shows the variation of the floating potential of the probe with the laser heating power. Starting from the floating potential $V_{fl} \cong -3.3$ V of the same but cold probe, with increasing heating power the floating potential rises. At a laser power of $P_L \cong 13$ W, the floating potential jumps up and reaches a final saturation of $V^*_{fl,em} = +8.8$ V for $P_L \geq 40$ W. This value lies about $2.9\,T_e$ above V_{fl}. We emphasize that Δ here has the same meaning as in the theoretical case (see Fig. 3a), *i.e.*, the difference between the actual value $V_{fl,em}$ and $\Phi_{pl} = 11.6$ V determined from the characteristic of the unheated probe.

As in the case of the emissive wire probe (section 3.1.1.), again we see here the discrepancy between this value and the saturation value of $V^*_{fl,em} = 8.8$ V, which is ascribed to the formation of negative space charge sheath around the emissive probe [18]. However, in contrast to the emissive wire probe in CASTOR, here $V^*_{fl,em}$ lies only about $0.68\,T_e$ below Φ_{pl}. This is in agreement with simulations [21]. Obviously this effect still needs further thorough investigations.

3.2. THE BALL-PEN PROBE

The other method to shift the floating potential of a probe towards the plasma potential is to reduce the electron saturation current. Coming back to Eq. (3), we see that the second term of this equation will also vanish for $I_{es} = I_{is}$. Obviously this cannot be achieved with a normal cold probe and especially not in an isotropic plasma. But in a strong magnetic field we can take advantage of the fact that the gyroradius of the electrons is much smaller than that of the ions. Also this is due to the much smaller mass of the electrons since the mean gyroradius is given by:

$$r_{e,i} = \sqrt{\frac{2T_{e,i}m_{e,i}}{e}}\frac{1}{B}. \tag{8}$$

So, for instance, in the CASTOR tokamak with a hydrogen plasma with $T_e = T_i = 10$ eV and $B = 1$ T the gyroradii for ions and electrons are approximately $r_i = 0.46$ mm and $r_e = 0.01$ mm, respectively.

In the 1960's, Katsumata and Okazaki invented a new type of probe, which was supposed to be sensitive only to ions [22, 23]. Indeed it was able to record

the ion energy distribution perpendicular to the magnetic field. The idea was that in a magnetic field the electrons can be shielded off from the cylindrical collector by a ceramic tube behind which the collector is retracted by a distance roughly corresponding to the average ion gyroradius. The collector was movable and was inserted with the surrounding tube perpendicular to the magnetic field. On a similar principle we have constructed an ion-sensitive tunnel probe by which the ion energy distribution function could be measured in CASTOR [24, 25].

To measure the plasma potential, we have developed Katsumata's idea further on in order to shield of not the entire electron current but an adjustable part of it [26, 27]. In order to make the transition between full electron collection and no electron collection smoother, the collector has a conical tip in contrast to the original by Katsumata and Okazaki [22]. Fig. 6 shows this probe, which is also inserted perpendicular to the magnetic field into the edge region of CASTOR. Since the collector can be shifted up and down inside the boron nitride tube similar to a ball-pen we have baptized the probe accordingly.

The coordinate h indicates the collector position with respect to the lower end of the BN tube: $h = 0$ means the tip lies exactly in this plane as also shown in Fig. 6. Positive values of h mean the collector is protruding; for negative values the collector is retracted into the BN tube. Obviously in this latter case the

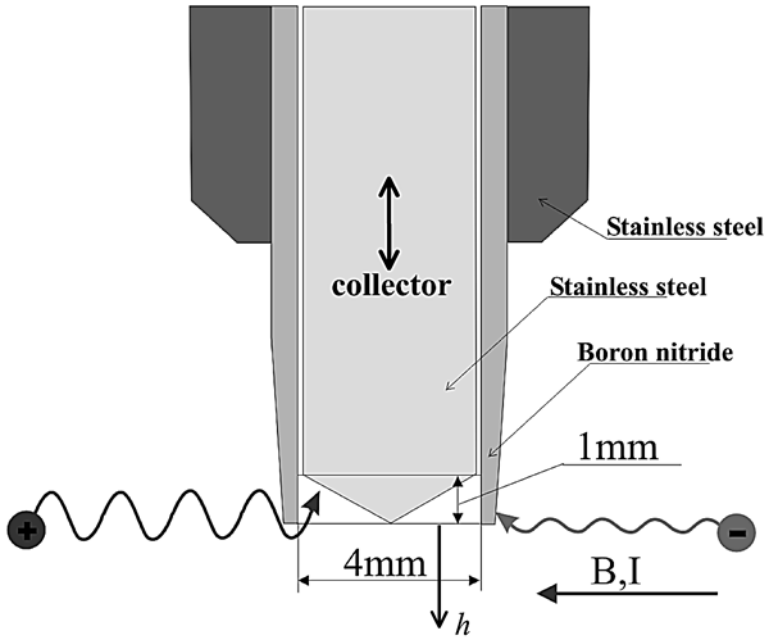

Fig. 6. – Schematic of the ball-pen probe. The collector can be shifted up and down on a shot-to-shot basis in CASTOR. The coordinate h indicates the position of the collector tip relative to the top cross section plane of the shielding BN tube.

electrons should not be able to reach the collector at all, whereas the ions can still pass by the shielding tube due to their larger gyroradius.

Coming back to Eq. (3), this can be rewritten as:

$$\Phi_{pl} = V_{fl} + T_e \ln\left(\frac{j_{es} A_e(h)}{j_{is} A_i(h)}\right). \tag{9}$$

Thus for V_{fl} becoming equal to Φ_{pl}, we have to postulate that

$$\frac{j_{es} A_e(h)}{j_{is} A_i(h)} = 1. \tag{10}$$

While we cannot change the current densities $j_{es,is}$ in the plasma, what we can do with the ball-pen probe is to vary the effective areas for electron and ion collection $A_{e,i}$, depending on h and of course on the magnetic field strength. Assuming a very strong magnetic field, from geometrical consideration, in the range $1 > h \geq 0$ mm, we have made estimates of the effective areas for electron and ion collection as functions of h, based on which the ratio A_e/A_i becomes:

$$\frac{A_e}{A_i} \cong \frac{h^2}{1.492 + 0.371 h^2}. \tag{11}$$

Estimates of the saturated current densities of the ions and electrons towards a probe in a typical CASTOR plasma with $n_e = n_i = 5\times10^{18}$ m^{-3} and $T_e = T_i = 10$ eV (now taking into account that the ions should have the ion acoustic velocity), we obtain a ratio of $j_{es}/j_{is} \cong 20$. Inserting this and Eq. (11) into Eq. (10) delivers $h \cong 0.27$ mm. This is within the expectations.

Fig. 7a,b shows similar graphs as Fig. 5a,b. Fig. 7a shows typical current-voltage characteristics of the ball-pen probe for three values of h. These measurements have been made at a radial position of $r = 7.5$ cm in the edge region of CASTOR, *i.e.*, slightly inside the last-closed flux surface, for purely ohmic discharges (this means that no edge biasing has been performed). For $h = 1.5$ mm (fully protruding collector) the characteristic looks like a typical characteristic of a cold probe. For $h = 0.6$ mm, where the collector is no longer fully exposed to the plasma, we see already a decrease of the electron saturation current with respect to the ion saturation current. And for $h = -1.0$ mm, both currents are almost equal. We emphasize, however, that here for better comparison the probe current has always been normalized to the value of I_{is} for $h = 1.5$ mm.

Fig. 7b shows the dependence of the floating potential of the probe on h (squares). Coming from the right-hand side, *i.e.*, for positive values of h, we first obtain a value of $V_{fl} \cong -11$ V. For $h = 1.0$ mm the floating potential begins to increase, reaching a maximum of about 24 V for $h = 0$. This value remains rather con-

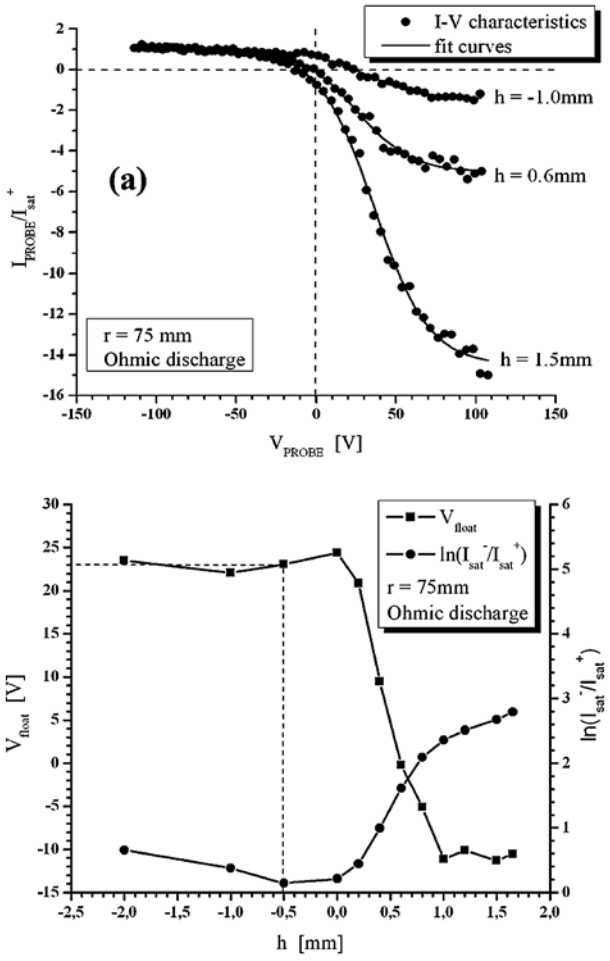

Fig. 7. – (a) I–V characteristics for various collector positions. h is negative when the collector is inside the shielding tube; (b) floating potential V_{fl} and $\ln(I_{es}/I_{is})$ with respect to h.

stant up to the left side of the graph for $h = -2.0$ mm. Even for smaller values of h we still are able to detect a clear value for the floating potential. From that we have to conclude that even then both particle species are able to reach the probe collector.

The circles in Fig. 7b show the behavior of the factor $\ln(I_{es}/I_{is})$ appearing in Eq. (3). As we have seen this quantity has to become zero in order to attain $V_{fl} = \Phi_{pl}$. For a normal cold probe in a magnetized hydrogen plasma this quantity is about 3 and is identical to $(V_{fl} - \Phi_{pl})/T_e$ (see also Eq. 6) [15]. This is also the value in Fig. 7b for $h \geq 1.7$ mm. Going to the left, $\ln(I_{es}/I_{is})$ decreases, reaching a minimum for $h = -0.5$ mm. This minimum is, however, not completely zero but about 0.2. Then it increases again a little bit.

The value of $V_{fl} \cong 23$ V for $h = -0.5$ mm has been taken as the value of the plasma potential. Further measurements have been performed by directly recording

the floating potential of this probe for this value of h. The fact that in this position the collector was not exposed to the direct flux of particles in the plasma, is very beneficial since such a probe could be used even in plasmas with a much stronger particle flux without danger for the collector.

The surprising fact that even for very much retracted collector, electrons and ions can still reach the collector, is tentatively explained by invoking an $\boldsymbol{E}\times\boldsymbol{B}$ drift where the electric field is formed between the plasma and the BN tube walls which are naturally on floating potential, *i.e.*, more negative than the plasma. When this $\boldsymbol{E}$-field is at an appropriate angle to the $\boldsymbol{B}$-field the resulting $\boldsymbol{E}\times\boldsymbol{B}$ drift would be more or less parallel to the tube axis and thus drive both particle species into the tube.

CONCLUSION

We have developed and discussed various types of plasma probes, by which a direct determination of the plasma potential is possible, even in the edge region of smaller toroidal fusion experiments. These probes are constructed in such a way that their floating potential yields an acceptably good measure of the plasma potential. One type is the emissive probe, of which we have presented the conventional emissive wire probe and the newly developed laser-heated emissive probe. In this case an electron emission current compensates the electron saturation current from the plasma. Another principle is used for the ball-pen probe which is based on the difference between the gyroradii of electrons and ions in a magnetic field. With these probes also the temporal development of the plasma potential can be recorded with all fluctuations, and arrangements are feasible, by which the electric field in various directions can be determined directly. A certain perturbation of the plasma by such a probe can unfortunately not be avoided. But this depends also on the size of the probes, and can still be further improved.

Acknowledgement. This work has been carried out within the Association EURATOM-ÖAW, EURATOM-IPP.ČR and EURATOM-IPP (Greifswald Branch). The content of the publication is the sole responsibility of its author(s) and it does not necessarily represent the views of the Commission or its services. The support by the Fonds zur Förderung der wissenschaftlichen Forschung (Austria) under grant No. P-14545 is acknowledged. The work was further supported by grant GA ČR 202/03/0786 (probe construction) and project AV K2043105 (tokamak operation), partially by INTAS project No. 2001–2056.

REFERENCES

1. F. Wagner, G. Becker, K. Behringer, D. Campbell, A. Eberhagen, W. Engelhardt, G. Fussmann, O. Gehre, J. Gernhardt, G. v. Gierke, G. Haas, M. Huang, F. Kerger, M. Keilhacker, O. Klübner, M. Kornherr, K. Lackner, G. Lisitano, G. G. Lister, H. M. Mayer, D. Meisel, E. R. Müller, H. Murmann, H. Niedermeyer, W. Poschenrieder, H. Rapp, H. Röhr,

F. Schneider, G. Siller, E. Speth, A Stäbler, K. H. Steuer, G. Venus, O. Vollmer, Z. Yü, *Regime of improved confinement and high beta in neutral-beam-heated divertor discharges of the ASDEX tokamak*, Phys. Rev. Lett. 49, 1408–1412 (1982).

2. S.-I. Itoh, K. Itoh, *Model of L to H-mode transition in tokamak*, Phys. Rev. Lett. 60, 2276–2279 (1988).
3. K. H. Burrell, T. B. Carlstrom, E. J. Doyle, D. Finkenthal, P. Gohil, R. J. Gröbner, D. L. Hillis, J. Kim, H. Matsumoto, R. A. Moyer, T. H. Osborne, C. L. Rettig, W. A. Peebles, T. L. Rhodes, H. St. John, R. D. Stambaugh, M. R. Wade, J. G. Watkins, *Physics of the L-mode to H-mode transition in tokamaks*, Plasma Phys. Control. Fusion 34, 1859–1869 (1992).
4. E. Holzhauer, G. Dodel, M. Endler, J. Gernhardt, L. Giannone, M. Manso, K. McCormick, V. Mertens, H. Niedermeyer, A. Rudyj, F. Serra, A. Silva, G. Theimer, P. Varela, F. Wagner, H. Zohm, *The H-mode in the ASDEX tokamak*, Plasma Phys. Control. Fusion 36, A3-A11 (1994).
5. R. Moestam, J. Weiland, *On the L to H mode transition and instabilities on the H mode barrier in tokamak plasmas*, Nucl. Fusion 42, 663–669 (2002).
6. P. H. Diamond and Y. B. Kim, *Theory of mean poloidal flow generation by turbulence*, Phys. Fluids B 3, 1626–1633 (1991).
7. C. Hidalgo, C. Silva, M. A. Pedrosa, E. Sánchez, H. Fernandes, C. A. F. Varandas, *Radial structure of Reynolds stress in the plasma boundary of tokamak plasmas*, Phys. Rev. Lett. 83, 2203–2205 (1999); C. Hidalgo, M. A. Pedrosa, E. Sánchez, R. Balbín, A. López-Fraguas, B. van Milligen, C. Silva, H. Fernandes, C. A. F. Varandas, C. Riccardi, R. Carrozza, M. Fontanesi, B. A. Carreras, L. García, *Generation of sheared poloidal flows via Reynolds stress and transport barrier physics*, Plasma Phys. Control. Fusion 42, A153–A160 (2000).
8. S. B. Korsholm, P. K. Michelsen, V. Naulin, J. Juul Rasmussen, L. Garcia, B. A. Carreras, V. E. Lynch, *Reynolds Stress and shear flow generation*, Plasma Phys. Control. Fusion 43, 1377–1395 (2001).
9. K. Burrell, *Effects of E×B velocity shear and magnetic shear on turbulence and transport in magnetic confinement devices*, Phys. Plasmas 4, 1499–1518 (1997); P. W. Terry, *Suppression of turbulence and transport by sheared flow*, Rev. Mod. Phys. 72, 109–165 (2000).
10. P. Balan, J. Adámek, I. Duran, M. Hron, C. Ioniță, E. Martines, R. Schrittwieser, J. Stöckel, M. Tichý, G. Van Oost, *Measurements of the fluctuation-induced flux with emissive probes in the CASTOR Tokamak*, Proc. 29th EPS Conf. Plasma Physics Control. Fusion, (Montreux, Switzerland, 2002), Europhys. Conf. Abst. 26B, 2.072-2.075 (2002).
11. P. Balan, J. A. Cabral, R. Schrittwieser, H. F. C. Figueiredo, H. Fernandes, C. Ioniță, C. Varandas, J. Adámek, M. Hron, J. Stöckel, E. Martines, M. Tichý, G. Van Oost, *Emissive Probe Measurements of the Plasma Potential Fluctuations in the edge of the ISTTOK and CASTOR Tokamaks*", 14th APS Topical Conf. High Temperature Plasma Diagnostics (Madison, Wisconsin, USA 2002) and Rev. Sci. Instrum. 74, 1583–1587 (2003).
12. C. Ioniță, P. Balan, R. Schrittwieser, H. F. C. Figueiredo, R. M. O. Galvao, C. Silva, C. A. F. Varandas, *An arrangement of emissive probe and cold probes for fluctuation and Reynolds stress measurements*, 15th Topical Conf. High-Temperature Plasma Diagnostics (San Diego, USA, 2004) and Rev. Sci. Instrum., in print; P. Balan, H. F. C. Figueiredo, R. M. O. Galvão, C. Ioniță, V. Naulin, J. J. Rasmussen, R. Schrittwieser, C. G. Silva, C. Varandas, *Measurements of the Fluctuation-Induced Flux and the Reynolds Stress in the edge region of ISTTOK*, Proc. 31st EPS Conf. Plasma Phys. (London, Great Britain, 2004), in print.
13. H. M. Mott-Smith, I. Langmuir, *The theory of collectors in gaseous discharges*, Phys. Rev. 28, 727–763 (1926).
14. I. Langmuir, *The interaction of electron and positive ion space charges in cathode sheaths*, Phys. Rev. 33, 954–989 (1929).

15. R. Schrittwieser, J. Adámek, P. Balan, M. Hron, C. Ioniță, K. Jakubka, L. Kryška, E. Martines, J. Stöckel, M. Tichý, G. Van Oost, *Measurements with emissive probes in the CASTOR tokamak*, Plasma Physics Control. Fusion 44, 567–578 (2002).
16. A. Siebenförcher, R. Schrittwieser, *A new simple emissive probe*, Rev. Sci. Instrum. 67, 849–850 (1996).
17. R. Schrittwieser, C. Ioniță, P. C. Balan, Jose A. Cabral, H. F. C. Figueiredo, V. Pohoață, C. Varandas, *Application of emissive probes for plasma potential measurements in fusion devices*, Contrib. Plasma Phys. 41, 494–503 (2001).
18. M. Y. Ye, S. Takamura, *Effect of space-charge limited emission on measurements of plasma potential using emissive probes*, Phys. Plasmas 7, 3457–3463 (2000).
19. R. Madani, C. Ioniță, R. Schrittwieser, G. Amarandei, P. Balan, T. Klinger, *A laser-heated emissive probe for fusion applications*, Proc. 31st EPS Conf. Plasma Phys. (London, Great Britain, 2004), in print.
20. C. M. Franck, O. Grulke, T. Klinger, *Mode transitions in helicon discharges*, Phys. Plasmas 10, 323–325 (2003).
21. K. Reinmüller, *Determination of the Plasma Potential using emissive probes – Implications from PIC simulations*, Contrib. Plasma Phys. 38, 7–12 (1998).
22. I. Katsumata, M. Okazaki, *Ion sensitive probe – a new diagnostic method for plasma in magnetized fields*, Japan J. Appl. Phys. 6, 123–124 (1967).
23. I. Katsumata, *A review of ion sensitive probes*, Contrib. Plasma Phys. 36S, 73–80 (1996).
24. P. Balan, R. Schrittwieser, J. Adámek, O. Bařina, P. De Beule, I. Ďuran, J. P. Gunn, R. Hrach, M. Hron, C. Ioniță, E. Martines, R. Pánek, J. Stöckel, G. Van Den Berge, G. Van Oost, T. Van Rompuy, M. Vicher, *Measurements of the parallel and perpendicular ion temperatures by means of an ion-sensitive segmented tunnel probe*, Contrib. Plasma Phys., in print.
25. J. P. Gunn, R. Schrittwieser, P. Balan, C. Ioniță, J. Stöckel, J. Adámek, I. Ďuran, M. Hron, R. Pánek, O. Bařina, R. Hrach, M. Vicher, G. Van Oost, T. Van Rompuy, E. Martines, *Tunnel probes for measurements of the electron and ion temperature in fusion plasmas*, Rev. Sci. Instrum., in print.
26. J. Adámek, J. Stöckel, M. Hron, J. Ryszawy, P. Balan, C. Ioniță, R. Schrittwieser, E. Martines, M. Tichý, G. Van Oost, *A novel approach to direct measurement of the plasma potential*, Proc. 21st Symp. Plasma Phys. Technol. (Prague, Czech Republic, 2004), in print.
27. J. Adámek, P. Balan, M. Hron, C. Ioniță, E. Martines, J. Ryszawy, R. Schrittwieser, J. Stöckel, M. Tichý, G. Van Oost, *Direct plasma potential measurements by a novel probe*, Proc. 31st EPS Conf. Plasma Phys. (London, Great Britain, 2004), in print.